

Photocurrent calculations in beryllium using a local dielectric model

R. K. Thapa

Department of Physics, Pachhunga University College, North Eastern Hill University, Aizawl 796 001, Mizoram, India

N. Kar

Department of Physics, North Bengal University, Darjeeling, Siliguri 734 430, West Bengal, India

(Received 24 June 1994; revised manuscript received 3 November 1994)

Photocurrent is calculated, using a local dielectric model, from the bulk (Fermi level) and surface states of beryllium for low photon energy range (≤ 30 eV). Free-electron wave functions are used in the matrix element for computing the photocurrent. The calculated data are compared with the experimental data.

Angle-resolved photoemission spectroscopy (ARPES) techniques have been used quite extensively in understanding the electronic structure of the surface and bulk of various solids.¹⁻⁴ Here both transitions between bulk electron bands and excitations of electrons located in surface-state bands have been detected, and a knowledge of the bulk and surface electron structure near and far away from the Fermi level obtained. The surface states detected are located in energy-band gaps obtained by projecting the three-dimensional band structure onto the two-dimensional surface Brillouin zone. This type of band gap was also found⁵ by using ARPES in the case of beryllium along the symmetry line $\bar{\Gamma}-\bar{M}$, with photon energy in the range 24–30 eV. A surface state was detected⁵ at $\bar{\Gamma}$ in the $\bar{\Gamma}_3-\bar{\Gamma}_4$ band gap, with the initial-state energy located at 2.8 eV. Bartynski *et al.*⁶ also measured the photon energy ($\hbar\omega$) dependence of the photoemission intensity in the case of beryllium. They measured the photoemission intensity which shows agreement poorer than was found in the case of aluminum. This may be due to the fact that aluminum is much more free-electron-like than beryllium. Here we use the free-electron model that was applied⁷ to the case of aluminum in calculating the photocurrent from the surface and bulk states of beryllium.

The photocurrent is calculated by using the golden-rule formula:

$$\frac{dj(E)}{d\Omega} = \frac{2\pi}{\hbar} \sum |\langle \psi_f | \mathcal{H} | \psi_i \rangle|^2 \delta(E - E_f) \delta(E_f - E_i - \hbar\omega) \times f_0(E - \hbar\omega) [1 - f_0(E)], \quad (1)$$

where \mathcal{H} is the perturbation responsible for photoemission by radiation of frequency ω , $\psi_i(E_i)$ refers to the initial-state wave function (energy), $\psi_f(E_f)$ refers to the final-state wave function (energy), and f_0 denotes the Fermi occupation function. We consider that photoemission takes place along the z axis, which is normal to the surface given by the $z = 0$ plane. We may therefore write \mathcal{H} as

$$\mathcal{H} = (e/mc) \left[A_\omega(z) \frac{d}{dz} + \frac{1}{2} \frac{d}{dz} A_\omega(z) \right], \quad (2)$$

where $A_\omega(z)$ is the vector potential. The model of Bagchi and Kar⁸ is employed to calculate $A_\omega(z)$. The metal is assumed to occupy all space to the left of the $z = 0$ plane. The response of the electromagnetic field is bulk-like everywhere except in the surface region defined by $-a/2 \leq z \leq a/2$. In this region, the model dielectric function is chosen to be a local one which interpolates linearly between the bulk value inside the metal and the vacuum value (unity) outside. The model⁸ frequency-dependent dielectric function is therefore given by

$$\epsilon(\omega, z) = \begin{cases} \epsilon(\omega) = \epsilon_1(\omega) + i\epsilon_2(\omega), & z \leq -a/2 \\ \frac{1}{2}[1 + \epsilon(\omega)] + [1 - \epsilon(\omega)] \frac{z}{a}, & -a/2 \leq z \leq a/2 \\ 1, & z \geq a/2. \end{cases} \quad (3)$$

For the local dielectric function $\epsilon(\omega, z)$, we use the experimental values given by Edwards.⁹ We consider p -polarized light to be incident on the surface plane, forming an angle θ_i with the z -axis. The calculated vector potential of interest $A_\omega(z)$ in the long-wavelength limit ($\omega a/c \rightarrow 0$) is

$$A_\omega(z) = \begin{cases} B, & z \leq -a/2 \\ B \frac{\epsilon(\omega)/[1 - \epsilon(\omega)]}{\frac{z}{a} + \frac{1}{2} \frac{[1 + \epsilon(\omega)]}{[1 - \epsilon(\omega)]}}, & -a/2 \leq z \leq a/2 \\ B\epsilon(\omega)z, & z \geq a/2, \end{cases} \quad (4)$$

where

$$B = \frac{\sin 2\theta_i}{[\epsilon(\omega) - \sin^2\theta_i]^{1/2} + \epsilon(\omega)\cos\theta_i},$$

and is a function of $\epsilon(\omega)$ and θ_i . To calculate the photocurrent, the matrix element in Eq. (1) can be evaluated by using the above expressions for the vector potential, for which the initial- and final-state wave functions are the ones used earlier.⁷

The plot of the photocurrent from the band states (Fer-

mi level) of beryllium is shown in Fig. 1 for a range of incident photon energy of 7–30 eV. The data used for this calculation are as follows: Fermi-level energy (E_F)=14.30 eV, work function (ϕ)=4.98 eV, scattering factor (α)=0.35, and surface width $a = 10.00$ (in a.u.). We find that our calculated photocurrent data showed only a peak at around 12 eV without going to a minimum at 19 eV, the plasmon energy ($\hbar\omega_p$) of beryllium. However, a minimum in the photocurrent takes place at a value of $\hbar\omega = 30$ eV, which is far greater than $\hbar\omega_p$. This might be due to assuming a low value for the scattering factor (α). A large value of α has some effect on the photocurrent behavior in beryllium, especially for $\hbar\omega > \hbar\omega_p$. For example, when $\alpha = 1.0$, we find¹⁰ the peak in the photocurrent at $\hbar\omega = 12$ eV followed by a minimum at around 19 eV, then a small peak of very low magnitude beyond it. This type of feature has also been found in the case of aluminum.⁷ Since we have assumed that beryllium is a free-electron type of metal (in fact, beryllium shows a large deviation from free-electron band structure), hence the necessary momentum for the photoexcitation is derived from the spatial variation of the vector potential. This is because the incident photon energy is too weak to photoexcite electrons lying in the Fermi level. Also, in free-electron metals, the bulk potential is too weak to produce the bulk photoeffect. This means that factor dA_ω/dz in \mathcal{H} is also important during photoemission in beryllium.

Further, to understand the occurrence of a peak in photocurrent at 12 eV, we also plotted dA_ω/dz as a function of z for photon energies of 7, 12, and 18 eV (see Fig. 2). We find that, in the surface region, maxima in dA_ω/dz occur only for a photon energy at 12 eV. For a photon energy at 7 eV, the peak in dA_ω/dz is shifted toward the vacuum side, whereas at 18 eV no such peak was found. This implied that the spatial variation of A_ω in the surface region for $\hbar\omega < \hbar\omega_p$ is responsible for maxima in photocurrent.

For the surface-state photocurrent calculation, the initial-state wave function $|\psi_i\rangle$ was replaced by a properly normalized Gaussian type of the wave function centered at the $z = z_0$ plane as used by Bagchi and Kar.⁸ By employing the same final-state wave function,⁷ the photo-

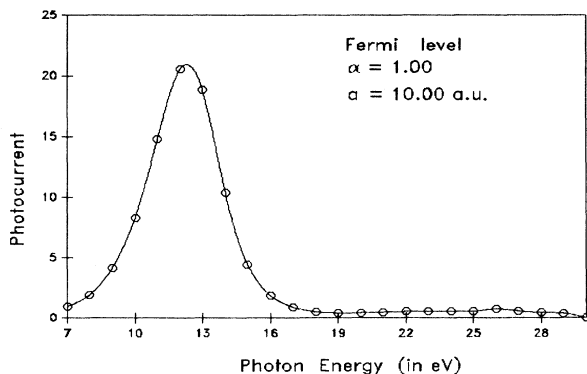


FIG. 1. Plot of photocurrent against photon energy from the Fermi level of beryllium.

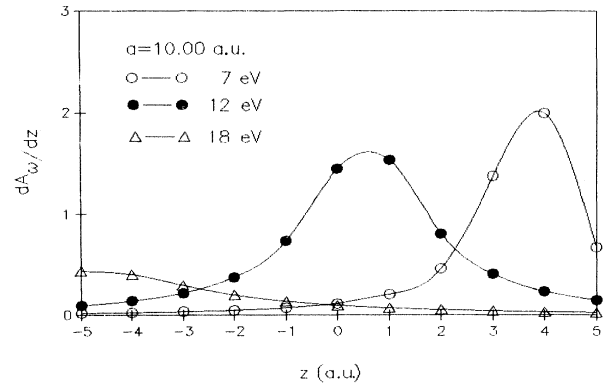


FIG. 2. Plot of $dA_\omega(z)/dz$ against z for photon energies at 7, 12, and 18 eV.

current from the surface state was evaluated using the following data: surface-state energy (E_i)=2.8 eV, $\beta = 2.00$, surface width (a)=10.00 a.u., and angle of incidence $\theta_i = 45^\circ$. The plot of the photocurrent against the photon energy is shown in Fig. 3 for locations of $|\psi_i\rangle$ at the surface ($z_0 = 0.0$) and at a distance $z_0 = -1.00$ and -2.00 a.u. from the surface toward the bulk side of the solid. In the surface region, we find a peak in photocurrent at $\hbar\omega = 12$ eV followed by a minimum at around 17 eV. There is again an enhancement in photocurrent at 26 eV. Bartynski *et al.*⁶ measured a strong emission near $\hbar\omega = 14$ eV with a suppression near 23 eV, and another peak at 30 eV. Thus we see that the behavior of the photocurrent in the surface region at values of $\hbar\omega$ below and above $\hbar\omega_p$ showed a qualitative agreement with the results of Bartynski *et al.*,⁶ but the peak in photocurrent curves (Fig. 3) continues to decrease for $\hbar\omega > \hbar\omega_p$ as the location of $|\psi_i\rangle$ is pushed further toward the bulk region with respect to the surface. Here we find that the shape and position of the experimental profile are reproduced quite well, but the agreement is not as good as was found in the case of aluminum.^{7,11} This may be due to the fact that aluminum is much more free-electron-like than beryllium, and is better described by jellium-model calculations.^{12,13}

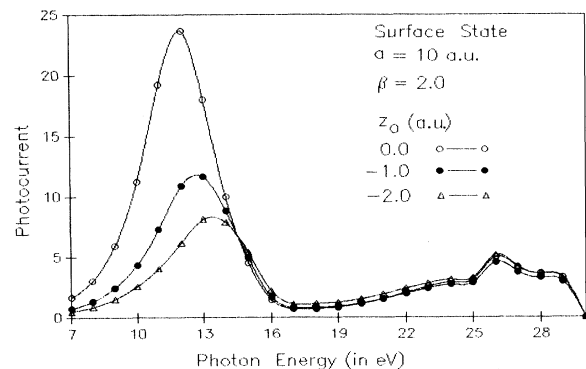


FIG. 3. Plot of photocurrent against photon energy from the surface state of beryllium for location of $|\psi_i\rangle$ at the surface and at a distance -1.00 and -2.00 a.u. from the surface.

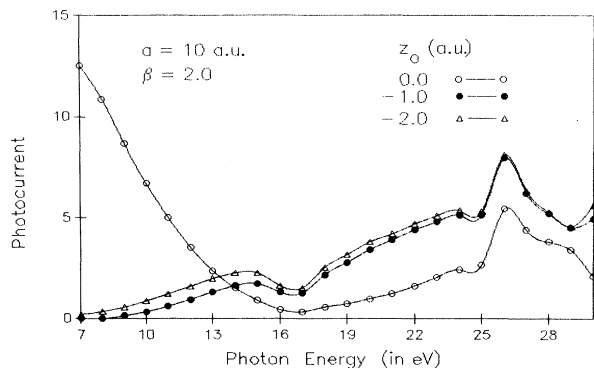


FIG. 4. Plot of photocurrent against photon energy using Fresnel field from the surface state of beryllium for location of $|\psi_i\rangle$ at the surface and at a distance -1.00 and -2.00 a.u. from the surface.

As further evidence of the occurrence of maxima in the photocurrent at 12 eV, we have also performed calculations with the same data as used for surface-state calculations in beryllium, but using the Fresnel refraction formula

$$A_\omega(z) = \begin{cases} B, & z < 0 \\ B\varepsilon(\omega), & z > 0, \end{cases} \quad (5)$$

and the same (free electron) wave functions.^{7,11} We found that the photocurrent curves for three values of z_0 showed neither a peak at 12 eV nor a minimum at the plasmon energy (Fig. 4). This means that photocurrent calculations with the Fresnel formula completely failed to reproduce the peak at 12 eV.

Feibelman¹³ used nonlocal optics and performed microscopic calculations (ignoring the local-field effects) of the spatial variation of the vector potential in the neighborhood of the jellium-vacuum interface. He used the Lang-Kohn potential barrier and evaluated $A_\omega(z)$ in terms of the conductivity tensor for photon energies below and above the plasmon energy. It was seen that $A_\omega(z)$ showed a peak below the plasmon energy with a minimum at $\hbar\omega_p$. Above $\hbar\omega_p$, such a peak in the surface region was not exhibited. Feibelman¹³ explained from nonlocal considerations that this had a direct relationship with the charge-density variation in the surface region, which he showed by plotting dA_ω/dz and dn_0/dz against photon energies below and above the plasmon energy. He found that in both cases the graph did show a peak in the surface region for $\hbar\omega < \hbar\omega_p$ which was attributed to the response of the solid to the electromagnetic field lo-

calized at the surface. However, for $\hbar\omega > \hbar\omega_p$, fluctuations of the induced charge could not be localized at the surface, because the induced plasmons transport the oscillating charges toward the interior of the solid, thereby reducing the healing length of the electrons. This, therefore, is the reason for the occurrence of minima in the photocurrent at a photon energy greater than the plasmon energy.

We have thus shown that with a simple model for the dielectric function, we can obtain a qualitative agreement with the experimental data. The calculations of Feibelman¹³ and Levinson, Plummer, and Feibelman,¹² employing the self-consistent jellium model for fields in the surface region, are more sophisticated, and their results are in better agreement with the experimental data. However calculations for jellium cannot be extended to more complicated cases, such as transition metals or semiconductors, while the model we have employed can be extended to these cases.^{14,15} Thus the qualitative agreement we obtain here in the case of beryllium and the previous application to the case of aluminum^{7,11} and tungsten⁸ gives us confidence to apply this model to photoemission calculations for other metals and semiconductors. However, for these cases, we can no longer use free-electron wave functions. We are working to combine a better description¹⁶ of the wave function with the field given by this model for photocurrent calculations from other metals.

There are shortcomings in this model for electromagnetic field employed here, for example, since experimentally measured dielectric functions are used as inputs. However, it gives results in reasonable agreement with the experimental data, and has the potential of being used for a number of metals and semiconductors. This is evident from the data reported for palladium,¹⁴ tungsten, and silicon^{15,17} by using this model, also incorporating the Thapa and Kar¹⁸ wave functions developed with the Krönig-Penney model. Though the model used for the calculations is elementary, it contains much of the essential physics compatible with the model. Any improvement in the model would require self-consistent calculation for the fields as well as for the initial and final states such as those performed by Feibelman¹³ for the spectral dependence of the cross section for aluminum Fermi level using jellium model.

Research was sponsored by the Department of Atomic Energy, India. R.K.T. is indebted to Dr. S. G. Davison, University of Waterloo (Canada), who provided the relevant literature, and to Mrs. Kamala for critically examining the manuscript.

¹U. O. Karlsson, G. V. Hansson, P. E. S. Persson, and S. A. Flodstrom, Phys. Rev. B **26**, 1852 (1982).

²G. V. Hansson and S. A. Flodstrom, Phys. Rev. B **18**, 1562 (1978).

³H. J. Levinson, F. Greuter, and E. W. Plummer, Phys. Rev. B **27**, 727 (1983).

⁴E. W. Plummer, Phys. Scr. T **17**, 186 (1987).

⁵U. O. Karlsson, S. A. Flodstrom, R. Engelhardt, W. Gadeka, and E. E. Koch, Solid State Commun. **49**, 711 (1984).

⁶R. A. Bartynski, E. Jensen, T. Gustafsson, and E. W. Plummer, Phys. Rev. B **32**, 1921 (1985).

⁷R. K. Thapa, P. Das, and N. Kar, Phys. Teacher **33**, 21 (1991).

⁸A. Bagchi and N. Kar, Phys. Rev. B **18**, 5240 (1978).

⁹Handbook of Optical Constants of Solids, edited by Edwards D.

- Pallik (Academic, New York, 1991), p. 429.
- ¹⁰R. K. Thapa (unpublished).
- ¹¹P. Das, R. K. Thapa, and N. Kar, *Mod. Phys. Lett. B* **5**, 65 (1991).
- ¹²H. J. Levinson, E. W. Plummer, and P. J. Feibelman, *Phys. Rev. Lett.* **43**, 952 (1979).
- ¹³P. J. Feibelman, *Phys. Rev. Lett.* **34**, 1092 (1975), *Phys. Rev. B* **12**, 1319 (1975).
- ¹⁴R. K. Thapa, *Phys. Status Solidi* **179**, 391 (1993).
- ¹⁵R. K. Thapa, P. Das, and N. Kar, *Mod. Phys. Lett. B* **8**, 361 (1994).
- ¹⁶P. Das, R. K. Thapa, and N. Kar (unpublished).
- ¹⁷R. K. Thapa and N. Kar, *Surf. Sci.* (to be published).
- ¹⁸R. K. Thapa and N. Kar, *Indian J. Pure Appl. Phys.* **26**, 620 (1988).